

# Adenovirally Transduced Bone Marrow Stromal Cells Differentiate into Pigment Epithelial Cells and Induce Rescue Effects in RCS Rats

Stefan Arnhold,<sup>1</sup> Peter Heiduschka,<sup>2</sup> Helmut Klein,<sup>1</sup> Yvonne Absenger,<sup>1</sup> Serkan Basnaoglu,<sup>1</sup> Florian Kreppel,<sup>3</sup> Sylvia Henke-Fahle,<sup>4</sup> Stefan Kochanek,<sup>3</sup> Karl-Ulrich Bartz-Schmidt,<sup>4</sup> Klaus Addicks,<sup>1</sup> and Ulrich Schraermeyer<sup>2</sup>

**PURPOSE.** To determine the potential of adenovirally transduced bone marrow stromal cells (BMSCs) to differentiate into retinal pigment epithelial-like cells and to evaluate possible rescue effects after transplantation into the retinas of Royal College of Surgeons (RCS) rats.

**METHODS.** Through a high-capacity adenoviral vector expressing either green fluorescent protein (GFP) or pigment epithelial-derived factor (PEDF), rat MSCs were transduced *in vitro* before subretinal transplantation into Wistar rats or, alternatively, RCS rats. Two months after cell injection, the rats were killed and the eyes enucleated. The eyes were then investigated light microscopically or processed for electron microscopic investigations. Cell differentiation and integration were analyzed immunocytochemically using antibodies against cytokeratin and the tight junction protein ZO-1. Electroretinography was performed 16 days after injection of cells, to check whether a functional rescue could be detected.

**RESULTS.** *In vitro* experiments in cocultured human MSCs and human RPE cells showed that MSCs adopted RPE-like characteristics. In grafting experiments, some rat MSCs integrate into the host RPE cell layer of Wistar and RCS rats, indicated by their hexagonal morphology. Subretinally transplanted cells express the epithelial marker cytokeratin and establish tight junctions with the host RPE cells. Furthermore, rescue effects can be demonstrated after grafting of vector-transduced and nontransduced MSCs in semithin sections of dystrophic retinas. Ultrastructurally, MSCs can be detected on top of host RPE and in close contact with photoreceptor outer segments phagocytosing rod outer segments.

**CONCLUSIONS.** Taken together, these results raise the possibility that MSCs have the potency to replace diseased RPE cells and deliver therapeutic proteins into the subretinal space to pro-

tect photoreceptor cells from degeneration. (*Invest Ophthalmol Vis Sci.* 2006;47:4121–4129) DOI:10.1167/iovs.04-1501

In the ongoing discussion of using stem cells for cell replacement strategies, the most promising group of stem cells are those isolated from the adult organism. Among these adult stem cells are the mesenchymal stem cells from the bone marrow stroma, which have recently experienced a high level of attention as they can be easily isolated and can be obtained in almost unlimited numbers. Bone marrow stromal cells (BMSCs) can be expanded through as many as 20 to 50 population doublings in approximately 10 weeks.<sup>1,2</sup> Recently, it has been reported that bone marrow cells differentiate into various cell types, including hepatocytes,<sup>3</sup> endothelial cells of the blood vessels,<sup>4</sup> cardiac muscle,<sup>5</sup> and skeletal muscle.<sup>6</sup> It has also been reported that MSCs differentiate into neural cells and astrocytes *in vitro*.<sup>7</sup> Furthermore, they differentiate into astrocyte-like cells *in vivo* when transplanted into the normal or ischemic brain.<sup>8–10</sup> In addition, in the case of the rat eye, it has been published that MSCs can differentiate into photoreceptor-like cells.<sup>11</sup>

In this investigation, we sought to investigate the differentiation potency of BMSCs into pigment epithelial cells, as degeneration of this cell population also affects photoreceptor cell survival in various degenerative diseases of the retina.

Most approaches investigating the therapeutic potency as well as the differentiation capacity of stem cells *in situ* have been performed in the Royal College of Surgeons (RCS) rat, which is a well-established model of RPE degeneration in humans.<sup>12–14</sup> In these animals, a genetic mutation determines the inability of RPE cells to phagocytose rod outer segments, which is followed by the degeneration of photoreceptor cells. In the RCS rat, subretinal RPE cell transplantation can rescue photoreceptor cell degeneration<sup>15–17</sup> Thus, subretinal<sup>18–20</sup> and intrachoroidal<sup>21</sup> transplantation of stem- and other cell types, such as iris pigment epithelial cells<sup>21</sup> and Schwann cells,<sup>18</sup> have shown beneficial influence on photoreceptor survival. Furthermore, it has also been shown that the subretinal injection of embryonic stem cells rescues photoreceptor cells from degeneration in this animal model,<sup>22</sup> suggesting that stem cells could be a promising tool for the treatment of retinal degeneration. However, a therapeutic concept involving embryonic stem cells, although tempting, remains highly controversial, as the cells can induce tumor formation.<sup>23</sup>

For the first time, we show that MSCs have the ability to adopt an RPE-like morphology after subretinal grafting into normal adult rats and into RCS rats. Furthermore, it can be shown that MSCs are able to induce significant rescue effects regarding the preservation of photoreceptor cell nuclei. These rescue effects can even be increased in the dystrophic rats by combining this with an *ex vivo* gene therapeutic option using an adenoviral vector carrying the sequence of the pigment epithelium-derived factor (PEDF). Altogether, our findings indicate a possible therapeutic option for the treatment of pho-

---

From the <sup>1</sup>Department of Anatomy I, University of Cologne, Cologne, Germany; the <sup>3</sup>Section for Gene Therapy, University of Ulm, Ulm, Germany; and the <sup>2</sup>Section of Experimental Vitreoretinal Surgery and the <sup>4</sup>Department of Vitreoretinal Surgery, University of Tübingen, Tübingen, Germany.

Supported by the European Commission IP EVI-GenoRet LSHG-CT-512036 and Ilse Palm Stiftung.

Submitted for publication December 20, 2004; revised May 17 and October 28, 2005, and April 7 and May 14, 2006; accepted July 24, 2006.

Disclosure: S. Arnhold, None; P. Heiduschka, None; H. Klein, None; Y. Absenger, None; S. Basnaoglu, None; F. Kreppel, None; S. Henke-Fahle, None; S. Kochanek, None; K.-U. Bartz-Schmidt, None; K. Addicks, None; U. Schraermeyer, None

The publication costs of this article were defrayed in part by page charge payment. This article must therefore be marked "advertisement" in accordance with 18 U.S.C. §1734 solely to indicate this fact.

Corresponding author: Stefan Arnhold, Department of Anatomy I, Joseph-Stelzmann Strasse 9, 50931 Köln, Germany 4786711; stefan.arnhold@uni-koeln.de.

toreceptor cell and visual loss originally caused by the degeneration of the RPE layer.

## MATERIAL AND METHODS

### Isolation and Cultivation of Mesenchymal Stem Cells

Rat mesenchymal stem cells were isolated from bone marrow aspirates from the femurs of male adult Wistar rats.

Cell material was diluted 1:1 with  $\alpha$ -MEM and filtered through a 70- $\mu$ m nylon mesh (Cell Strainer, Falcon; BD Biosciences, Franklin Lakes, NJ). The resultant cell suspension was layered on top of a 15-mL single-density gradient (Ficoll-Paque Plus; GE Healthcare, Uppsala, Sweden) and centrifuged for 30 minutes at 800g at room temperature. The supernatant and interface were combined, diluted to approximately 50 mL with PBS (0.1 M), and centrifuged for 10 minutes at 800g. After the supernatant was discarded, the pellet was suspended in 1 mL medium. The nucleated cells were counted; suspended at a concentration of  $1 \times 10^7$ /mL in growth medium ( $\alpha$ -MEM supplemented with 2 mg/mL L-glutamine, 50  $\mu$ g/mL streptomycin, and 20% (vol/vol) of non-heat-inactivated fetal calf serum); and plated at  $3 \times 10^6$ /cm<sup>2</sup> in 100-mm culture dishes (Falcon; BD Biosciences). The cells were incubated for 3 days, and the nonadherent cells were removed by replacing the medium in three washing steps. After the cultures reached confluence, the cells were lifted by incubation with a cell-detachment enzyme (Accutase; PAA Laboratories, Cölbe, Germany) at 37°C for 3 to 4 minutes. They were diluted and plated at a density of 2000 cells/cm<sup>2</sup> in 100-mm culture dishes.

### Construction of HC-Ad Vectors and Cell Labeling

The high-capacity adenoviral vector (HC-Ad) was generated as previously described.<sup>24</sup> The HC-Ad.PEDF was constructed to express the human PEDF carrying a C-terminal 6-His tag. The vector HC-Ad.FK7 expressing enhanced GFP (EGFP) has been described.<sup>24</sup> BMSCs were infected with a stock AdV concentration of  $2 \times 10^6$  infection units/ $\mu$ L, corresponding to 50 multiplicities of infection (MOI) for a single cell. Transduction efficiency was analyzed 24 hours after transduction by determining the population of cells with EGFP expression within the total cell population labeled by the Hoechst dye nuclear stain.

Alternatively, as a control, cells were labeled using the cell membrane dye PKH 67 (Sigma-Aldrich, Deisenhofen, Germany).

For the ultrastructural analysis of transplanted BMSCs in the recipient retinas, they were labeled in culture with 5 nm colloidal gold (Sigma-Aldrich) 48 hours before subretinal transplantation. Analysis of successful gold labeling was performed *in vitro* using the silver enhancement kit (Sigma-Aldrich), yielding a black staining of gold labeled cells.

### Coculture of Human BMSCs and Human RPE Cells

For the coculture experiments, human BMSCs were isolated from patients undergoing total hip arthroplasty and cultivated according to the procedures described for the rat BMSCs. Before cocultivation, human BMSCs were transduced by using a combined HC-Ad vector carrying the sequences for GFP as well as for PEDF for 48 hours. RPE cells were obtained from a 52-year-old female patient who died after an apoplexy. All samples were obtained according to the ethical recommendations of the German Transplantation Law, with the approval of the Medical Ethics Committee, Cologne University, and in compliance with the Declaration of Helsinki.

RPE cells were cultivated in DMEM containing 10% (vol/vol) FCS and 1% (vol/vol) penicillin-streptomycin-ampotericin B (PSA) in a chamber slide at a density of 5000 cells per chamber. After 7 days in culture, 3000 mesenchymal stem cells were plated on top of the monolayer of RPE cells. Both cell types were cultivated for another 7 days. During the period of coculture, the morphology of mesenchymal stem cells was studied daily. After a 7-day period, cells were fixed in 4%

PFA in 0.1 M PBS and transferred for immunocytochemical investigations.

### Animals, Transplantation, and Flatmount Preparation

All procedures were performed in accordance with the ARVO Statement for the use of Animals in Ophthalmic and Vision Research. With a 30-gauge needle (Hamilton, Reno, NV), vector-transduced mesenchymal stem cells were injected into the superior subretinal space of the right eye of either anesthetized adult Wistar rats or 3-week-old RCS rats. Rats were anesthetized with an injection of ketamine-zylazine. The needle passed through the sclera, and 60,000 cells in 0.5  $\mu$ L medium were injected.

For sham operations, the same volume of Hanks' balanced salt solution (HBSS) was injected.

To exclude false-positive cell tagging by the possible occurrence of free vector particles, four animals received injections of BMSCs that were labeled by the membrane dye PKH67 before grafting instead of using the GFP vector.

In all experimental groups, the retinas were examined funduscopically with a stereomicroscope (Leitz, Wetzlar, Germany) after the injection, and eyes showing massive subretinal hemorrhage, vitreous hemorrhage, or large retinal detachments were excluded. Two months after transplantation, the eyes were enucleated and fixed in 4% PFA in 0.1 M PBS, and flatmounted preparations of the retina including the RPE layer were examined. To detect injected cells and to determine the extent of the transplant site, the flatmounts were examined and photographed by fluorescence microscopy (Axiophot; Carl Zeiss Meditec, Oberkochen, Germany).

### Immunohistochemical Staining Procedures

For the investigation of cytokeratin in BMSCs that had been cocultivated with human RPE cells, cell cultures were fixed after rinsing in 0.1 M PBS in 4% PFA. Cells and wholemount preparations were treated with blocking antibodies of 2% goat serum and 5% FBS for 30 minutes. In experiments requiring the labeling of collagen and vimentin, the cells were further treated with 0.025% Triton X-100 for 30 minutes and rinsed in PBS.

The following primary antibodies were used: anti-pan cytokeratin, mouse monoclonal antibody (1:1000; Sigma-Aldrich); anti-ZO-1 mouse monoclonal antibody (1:200; Chemicon, Hofheim/TS, Germany); anti-retinol binding protein mouse monoclonal antibody (1:1000; Acris Antibodies, Hiddenhausen, Germany); and anti-GFAP polyclonal antibody (1:1000; Progen Biotechnik, Heidelberg, Germany).

Incubations were performed overnight at 4°C. The secondary antibody was Cy3- or CY2-conjugated affinity-purified goat anti-mouse or anti-rabbit IgG (1:1000; Rockland, Gilbertsville, PA).

### Light and Electron Microscopy

For light (semithin sections) and electron microscopic investigations, the enucleated eyes were processed as follows. After removal of the corneas, the eyes were fixed overnight at 4°C in glutaraldehyde (4% solution in 0.1 M cacodylate buffer [pH 7.4]). Fluorescent areas in flatmount preparations were excised and postfixed with 1% osmium tetroxide at room temperature in 0.1 M cacodylate buffer for 3 hours, stained en bloc with uranyl acetate. Dehydration was then performed by a series of incubations in the following order: ethanol 50% (30 minutes), ethanol 70% (overnight), ethanol 96% (three times for 20 minutes each), absolute ethanol (three times for 20 minutes each), acetone (three times for 20 minutes each) and acetone+Araldite (overnight). The eyes were then embedded in Araldite for 48 hours. The blocks were sectioned semiserially in 0.7- $\mu$ m-thick sections on a microtome (Reichert Ultracut R; Leitz) and stained using the methylene blue dye. Rescue effects were quantified by using a light microscope (Axiophot; Carl Zeiss Meditec).

Preserved photoreceptor nuclei were counted at a magnification of 400 $\times$ . To gain statistically relevant results in each experimental group,

we used 10 animals. Only the right eyes were used for cell injections; the left eyes served as the untreated control. The evaluation was performed by masked investigators in three independent sections of each eye throughout the experimental groups.

Ultrathin sections (70 nm) were stained with uranyl acetate and lead citrate and observed under an electron microscope (model 902 A; Carl Zeiss Meditec).

### Deconvolution Microscopy

Digital slicing was performed with an inverted microscope (Axiovert 100M; Carl Zeiss Meditec) with an oil-immersion objective (model 63 Planapochromat; Carl Zeiss Meditec) and band-pass filter sets for Cy2 and Cy3 (AHF, Tübingen, Germany) without overlap in the fluorescence emission spectrum, and the accompanying software package (KS 400; Carl Zeiss Meditec). Each specimen was acquired as an image stack with 64 planes. The distance of the image planes was set to 100 nm to assure proper oversampling of the optical resolution for the subsequent iterative deconvolution process.

### Evaluation of Rescue Effects in Semithin Sections

The numbers of photoreceptor rows in the ONL were measured over a distance of 300  $\mu\text{m}$  of the retina adjacent to the grafting site. The number of photoreceptor rows was the average of three measurements counting rows of nuclei of preserved photoreceptor cells. Data analysis and statistics were performed on computer (Excel; Microsoft, Redmond, WA.) Data are given as mean  $\pm$  SEM. Comparison between two groups were made using Student's *t*-test. For all statistical tests *P* < 0.05 was taken as significant.

### ELISA Investigations for the Detection of PEDF in Cell Culture Supernatants

An ELISA assay was performed on BMSCs and conditioned medium to investigate whether these cells endogenously express PEDF and whether they secrete this factor into the cell culture medium. For the assay, flat-bottomed 96-well plates were coated with mouse anti-human PEDF antibody (lot no. 22070101; Chemicon) which binds soluble PEDF from the supernatants. For the analysis, flat-bottomed 96-well plates were coated with an anti-PEDF monoclonal antibody that binds soluble PEDF from the supernatants. The captured PEDF was bound by a second specific monoclonal antibody. After washing, the amount of specifically bound monoclonal antibody was detected with a species-specific antibody conjugated to horseradish peroxidase. After incubation with chromogenic substrates for peroxidases, the intensity of the developed color was measured photometrically. A standard curve was prepared with 2.5S PEDF standard by assaying parallel wells containing known amounts of the standard.

### Reverse Transcription–Polymerase Chain Reaction

Total RNA was isolated from mesenchymal stem cell cultures (RNeasy Mini Kit; Qiagen, Hilden, Germany). RNA (2  $\mu\text{g}$ ) was incubated with DNase I (Invitrogen, Karlsruhe, Germany), to remove DNA contamination. The procedures were performed according to the manufacturer's protocol. The RNA was reverse transcribed to first-strand cDNA with Moloney murine leukemia virus reverse transcriptase (Invitrogen) in a 50- $\mu\text{L}$  reaction mixture using an Oligo(dT)<sub>18</sub> primer (MWG Biotech, Ebersberg, Germany). PCR was performed with a thermocycler (Primus 96 Plus; MWG) in a volume of 50  $\mu\text{L}$  containing 4  $\mu\text{L}$  reverse transcribed product, by using the following specific primers: human PEDF (forward primer, 5'-CAAGAGTGCCCTCCCGGATCG-3'; reverse primer 5'-CCTTGAAGTGCGCCACACCG-3') and rat PEDF (forward primer, 5'-GATGACCCCTTCTCAAGGCC-3'; reverse primer, (5'-TCAGGGGCAGTAACAGAGGCA-3').

PCR was performed in a 50- $\mu\text{L}$  volume using 2.5-U *Taq* polymerase (BioTherm; Genecraft, Lüdinghausen, Germany). The reaction was performed for 34 cycles of 1 minute denaturation at 94°C, 1 minute

annealing at 60°C, and 1.5-minute elongation at 72°C. The PCR amplification was followed by a 10-minute final extension at 72°C. The generated PCR amplification products were separated by electrophoresis in a 2% agarose gel stained with ethidium bromide.

## RESULTS

### Coculture Experiments with Human BMSCs and Human RPE Cells

To show the differentiation potential of human BMSCs into RPE-like cells, coculture experiments using human BMSCs and human RPE cells were performed.

Deconvolution microscopy of these coculture experiments revealed that after a 7-day cocultivation period on chamber slides, adenovirally transduced BMSCs exhibited the typical morphologies of RPE cells in vitro. Furthermore, they could be observed in close contact to their neighboring RPE cells showing intracellular granules, possibly pigment granules, similar to their RPE counterparts (Figs. 1a, 1b). Immunocytochemical investigations revealed the expression of the epithelial marker cytokeratin in the cocultivated GFP-labeled BMSCs (Figs. 1c–e), indicating a differentiation capacity of mesenchymal stem cells to RPE-like cells in the human system.

### Subretinal Transplantation of BMSCs in Wistar Rats

GFP-labeled mesenchymal stem cells were injected microsurgically into the subretinal space of adult Wistar rats to study their adaptive quality and integrative potency in the recipient tissue of the retina. Transplantation success was determined by detection with a stereofluorescence microscope of GFP expression in the fundus of the eye directly after cell injection (Fig. 2a).

After a survival time of 2 months, the animals were killed and the eyes enucleated. BMSCs were easily identified because of their GFP expression in flatmounted preparations (Fig. 2b). Cells showed an integrative potential within the retinal pigment epithelium, exhibiting the typical hexagonal morphology of RPE cells.

After alternative labeling of mesenchymal stem cells using the membrane dye PKH67 instead of the adenoviral vector, false-positive cell tagging by the possible occurrence of free vector particles could be excluded. Also, under these labeling conditions, typical hexagonal morphologies of green fluorescent cells could be detected within the RPE layer (not shown).

Using immunocytochemical techniques, according to the local RPE cells, transplanted mesenchymal stem cells also expressed the epithelial protein cytokeratin (Figs. 2c–e). Injected mesenchymal stem cells were connected to their neighboring RPE cells by tight junctions, as shown by the expression of the tight junction protein ZO-1 (Figs. 2f, 2g). Neither tumor formation nor signs of an immunologic reaction after cell implantation were visible (not shown).

### Subretinal Transplantation of Mesenchymal Stem Cells in Dystrophic RCS Rats

After transplantation of BMSCs into the subretinal space of RCS rats, donor cells were clearly identifiable by their endogenous GFP expression. Similar to the situation in the nondystrophic Wistar rat, most cells were particularly situated within the layer of local RPE cells (Fig. 3a). BMSCs also differentiated into pigmented cells (Fig. 3b), and, moreover, analogous to the setting in Wistar rats, cells exhibited the expression of cytokeratin (Fig. 3c). Furthermore, they expressed the tight junction protein ZO-1 (Figs. 3d–f). In semithin sections of RCS retinas after grafting of BMSCs, they were detectable on top of

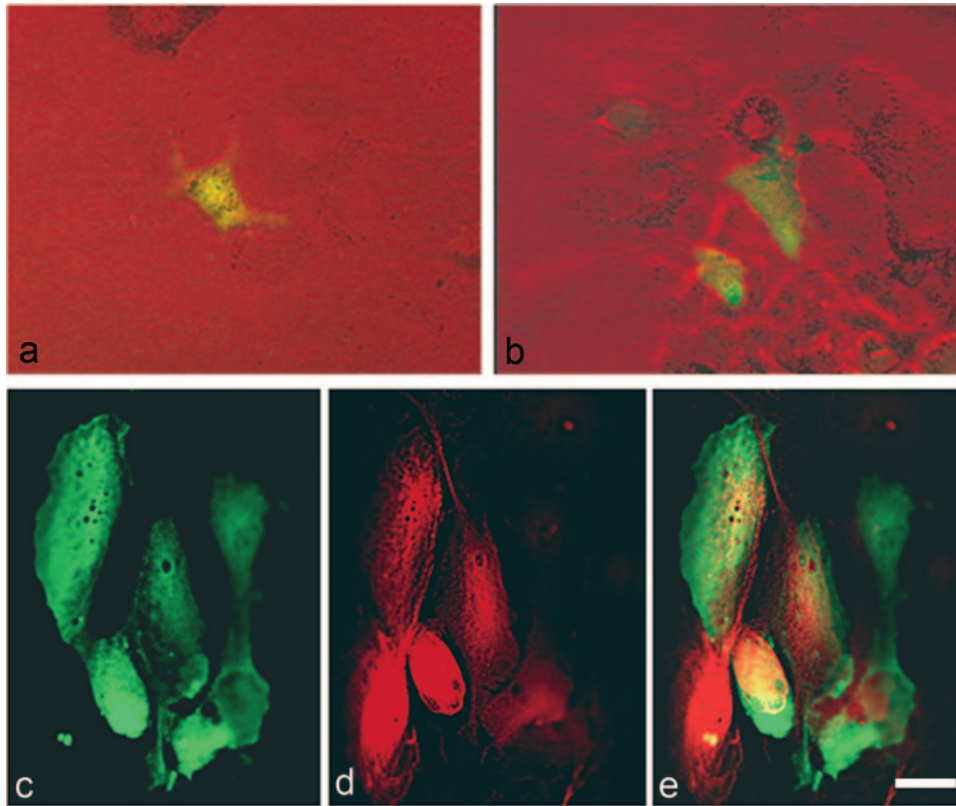


**FIGURE 1.** Coculture experiments of human BMSCs and human RPE cells. (a, b) GFP vector-transduced BMSCs showed morphologies similar to those of RPE cells and exhibit granules. (c) As analyzed by deconvolution microscopy, GFP vector-transduced BMSCs (d) expressed the epithelial marker cyokeratin in coculture with RPE cells, as shown by cyokeratin immunocytochemistry; (e) merged image. Scale bars: (a, b) 20  $\mu\text{m}$ ; (c-e) 10  $\mu\text{m}$ .

the RPE layer (Fig. 3g). In rare cases, injected cells also infiltrated the neuronal retina after transplantation of BMSCs into the dystrophic retinas of RCS rats, displaying typical morphologies of glial cells without actually expressing the glial marker GFAP (Fig. 3h). The antibody against the retinol binding protein showed that there was no immunoreactivity to be detected within transplanted BMSCs (data not shown).

### Effects of BMSCs on Photoreceptor Survival in RCS Rats

Two months after subretinal injection of BMSCs into the dystrophic eyes of RCS rats, marked rescue effects could be detected in semithin sections of the appropriate retinas. Whereas hardly any photoreceptor nuclei were present in the control eyes of nontreated animals, several rows of photoreceptor nuclei were preserved adjacent to BMSCs transplants that were either transduced by the GFP or the PEDF vector in vitro before cell injection (Fig. 4).

In evaluating the rows of preserved photoreceptor cells facing transplanted BMSCs after transduction with the adenoviral vector carrying the GFP sequence, we found that the preserved outer nuclear layer was still  $4.3 \pm 2.8$  cells deep compared with  $0.4 \pm 0.5$  row of cells in the untreated animals ( $P \leq 0.05$ ) and to  $1.4 \pm 0.8$  rows ( $P \leq 0.05$ ) in the sham-surgery group. After transplantation of the PEDF vector transduced BMSCs, there was a slight but insignificant increase in the number of cell rows ( $5.4 \pm 2.6$ ) compared with the GFP vector transduced BMSCs (Fig. 5). In the sections of both experimental groups using GFP or PEDF vector-transduced BMSCs, the area of preserved photoreceptor cells covered the whole width of the section (2000  $\mu\text{m}$ ).

Electron microscopic investigation of retinas after MSC grafting confirmed the observations at the light microscopic level in semithin sections. In the retina of wild-type animals, transplanted cells can be unequivocally identified between the

RPE layer and photoreceptor outer segments using the colloid gold labeling technique. These gold-labeled cells were identifiable as a second layer of cells on top of the RPE cells (Figs. 6a, 6b).

There were close contacts of outer segments and integrated gold labeled BMSCs (Fig. 6c). In retinas of dystrophic RCS rats after transplantation, BMSCs were also detectable on top of or between RPE cells. Normally, BMSCs can be detected in phagocytosed rod outer segments (Fig. 6d). The occurrence of several rows of preserved photoreceptor cell nuclei in our ultrastructural investigations after BMSC transplantation into RCS rats indicate a rescue effect on photoreceptor cell nuclei after subretinal BMSC transplantation (Fig. 6e).

### Evaluation of PEDF Synthesis by BMSCs

The ELISA assay performed to determine PEDF in the cell culture supernatants of mesenchymal stem cells revealed a mean concentration of 78.2 pg/mL in the medium of cultivated mesenchymal stem cells, compared with 100 ng/mL in the supernatant of RPE cells. Furthermore, with RT-PCR, transcripts of PEDF could be detected in rat mesenchymal stem cells as well as in human mesenchymal stem cells of different passages obtained from different patients (Fig. 7).

### DISCUSSION

Stem cells of different origin are said to have great potential for the treatment of degenerative diseases, including those of the retina. Bone marrow-derived mesenchymal stem cells are among the stem cells suitable for such a therapeutic option. These cells offer the great advantage of autologous availability, avoiding graft rejections as well as any ethical concerns associated with other stem cell populations (for review, see Barker and Widner<sup>25</sup>). As vision loss due to an induced deterioration of photoreceptor cells may be caused by a continuous degen-

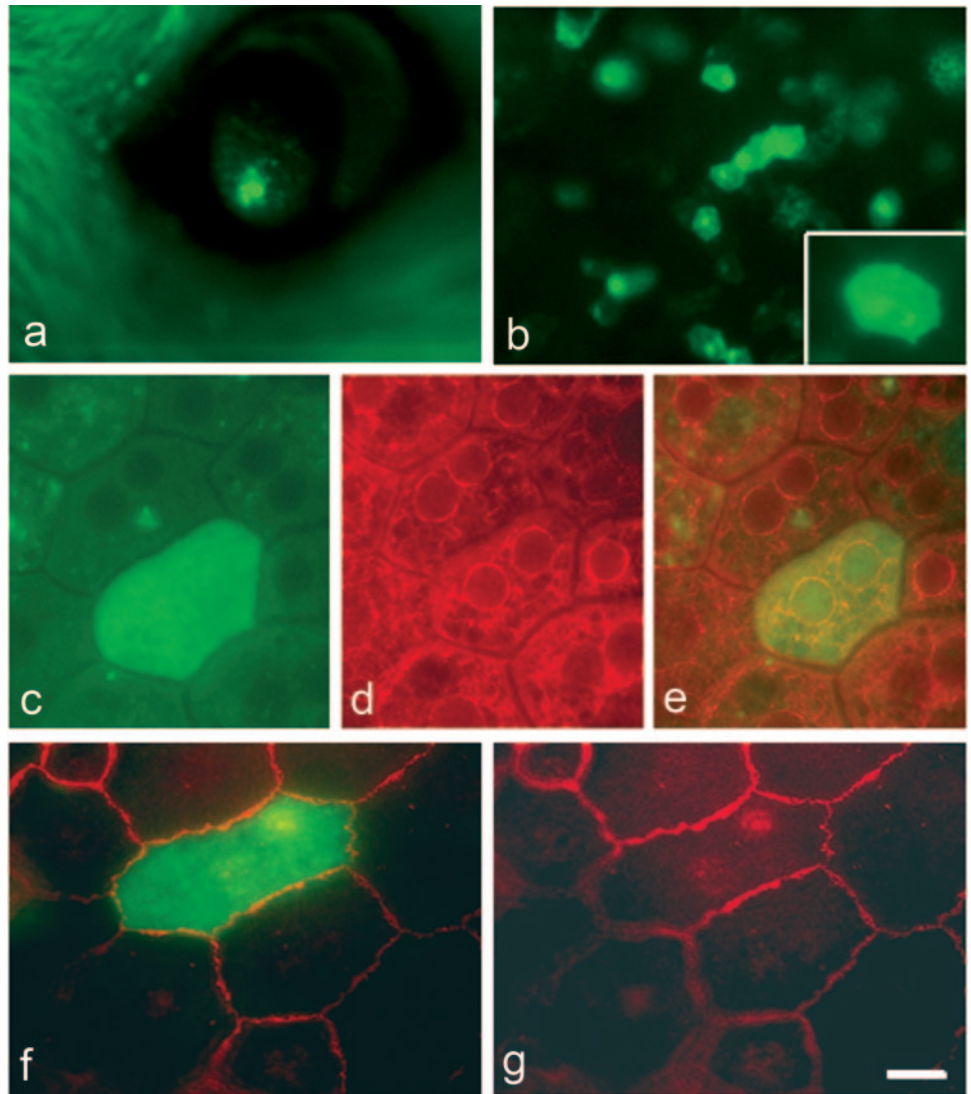


**FIGURE 2.** Vector transduced BMSCs after injection into the subretinal space of adult Wistar rats. (a) Stereomicroscopic detection of GFP expressing BMSCs in the fundus of transplanted animals. (b) Identification of BMSCs in the layer of the retinal pigment epithelium by their vector induced endogenous GFP expression. *Inset:* higher magnification of (b). (c) Cells showed the typical hexagonal morphologies of RPE cells and (d) expressed the epithelial marker cytokeratin, similar to the surrounding RPE cells; (e) merger of images (c) and (d). (f, g) RPE cells made contacts with the neighboring cells via the formation of tight junctions as shown by the expression of ZO-1 (red). Scale bars: (a) 1000  $\mu\text{m}$ ; (b) 40  $\mu\text{m}$ ; (*inset*) 15  $\mu\text{m}$ ; (c, d-f) 7  $\mu\text{m}$ .

eration of RPE cells,<sup>26</sup> we sought to investigate the integrative capacity of BMSCs within the RPE cell layer in our current approach. Moreover, we wanted to study a possible transdifferentiation potential of BMSCs into RPE-like cells.

The presented data reveal that subretinally transplanted BMSCs show a tendency of a morphologic integration within or on top of the RPE cell layer of normal Wistar rats as well as in the dystrophic retinas of RCS rats. After adenoviral transduction, the cells stably express the GFP reporter for the whole experimental period (2 months) without showing any adverse effects such as tumor formation. This circumstance is rather important in the light of reports about the occurrence of gastric cancer after transplantation of BMSCs in mice with *Helicobacter* infection.<sup>27</sup> There is also no indication of any immunologic reactions caused by BMSCs in the recipient tissue in our experiments. Of note, it has been shown in this context that these mesenchymal stem cells even seem to downregulate allogenic immune cell responses, that may generally lead to a reduction of transplantation complications such as rejection.<sup>28</sup>

Furthermore, cells show some of the typical characteristics of RPE cells in our grafting experiments. They adopt the hexagonal morphology of RPE cells, and, after transplantation, BMSCs even express the epithelial marker cytokeratin as analyzed by immunohistochemistry.

Similar to the RPE cells of the recipient tissue, BMSCs make contacts with adjacent RPE cells as shown by the expression of the tight junction protein ZO-1.

Rescue effects can be observed after transplantation of either GFP or PEDF vector-transduced BMSCs by preserving several layers of photoreceptor cells. Up to now, there have been several studies investigating the effect of either intraocular injection of neurotrophic factors such as bFGF<sup>29</sup> or cell replacement strategies for the substitution of degenerated RPE cells. Among these strategies, there have been attempts at direct substitution of RPE cells.<sup>30-32</sup> However, with RPE cells, there seems to be a donor age dependence in rescue effects. Thus, it could be shown that adult RPE cells induce a much lesser rescue effect than do neonatal cells.<sup>33</sup>

Furthermore, RPE-related cells such as autologous iris pigment epithelial cells have been used with variable success.<sup>20,34,35</sup>

Particularly in RPE cells, it can be demonstrated that genetically modified cells using a PEDF-expressing adenoviral vector produce more pronounced rescue effects<sup>35</sup> than after transplantation of nontransduced cells,<sup>20</sup> suggesting that PEDF as a neurotrophic factor has the potency to protect photoreceptor cells from degeneration in the RCS rat. Data from our experiments using mesenchymal stem cells reveal that these cells

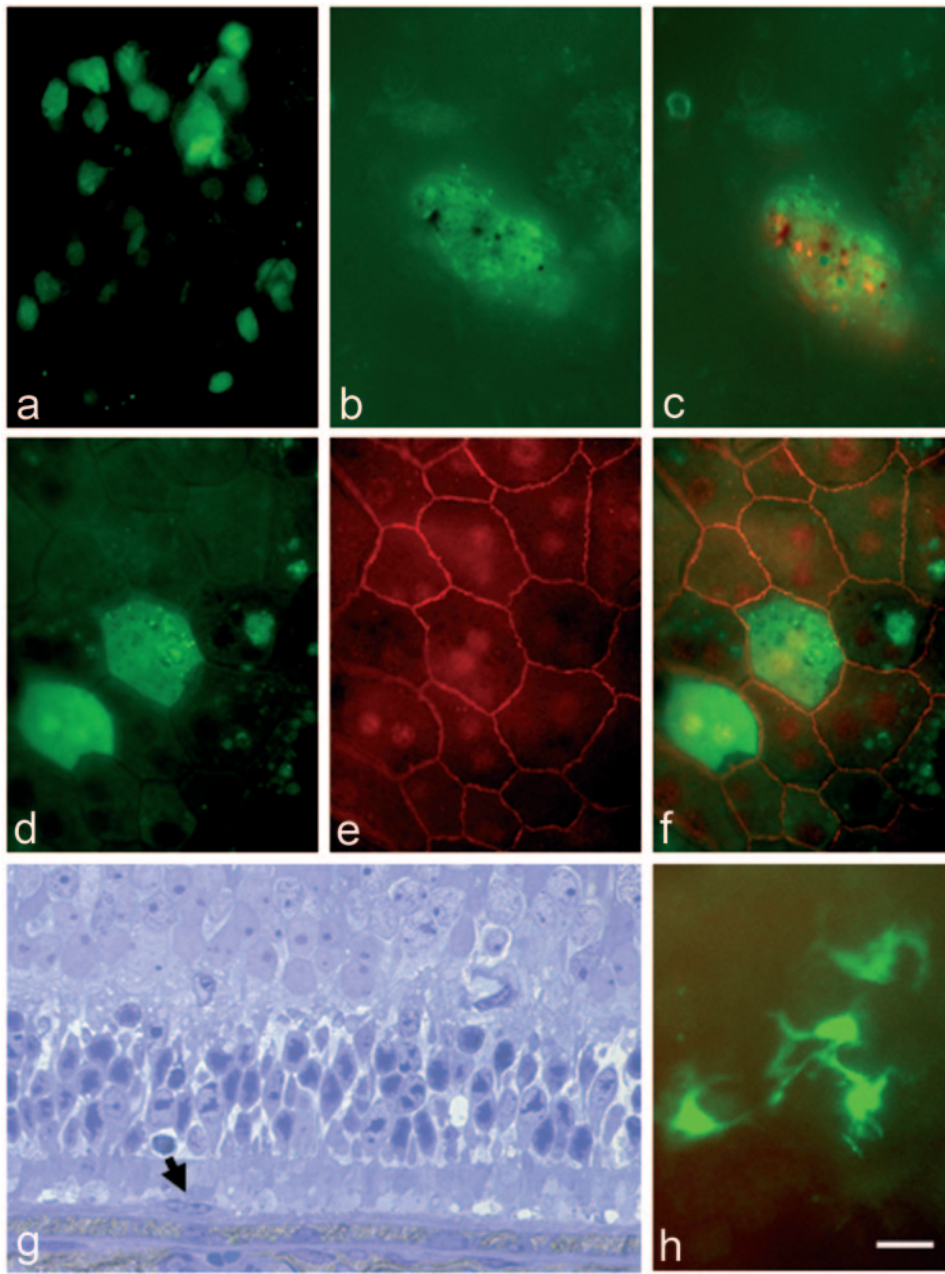


**FIGURE 3.** Transplantation of BMSCs in juvenile RCS rats. **(a)** After subretinal engraftment of GFP-expressing BMSCs into RCS rats, cells integrated within the layer of RPE and showed morphologies similar to those in wild-type animals. **(b)** GFP-expressing cells **(c)**, the expression of the epithelial protein cytokeratin (*red*). **(d)** GFP-expressing cells **(e, f)** formed contacts with neighboring cells, as shown by the expression of ZO-1. **(g)** In semithin sections transplanted BMSCs were detected frequently on top of the RPE cell layer in the RCS rats (*arrow*). Also note the layer of preserved photoreceptor cells. **(h)** In some cases, GFP-expressing BMSCs were also detectable in the neural retina, displaying typical morphology of glial cells. Scale bars: **(a)** 40  $\mu\text{m}$ ; **(b, c)** 10  $\mu\text{m}$ ; **(d-h)** 20  $\mu\text{m}$ .

already have the potency to rescue photoreceptor cells without genetic modification. These results may be attributed in part to the endogenous PEDF synthesis by these cells, as shown

by ELISA analysis in the supernatants of BMSCs as well as by our RT-PCR investigations. However, as the synthesis of PEDF by mesenchymal stem cells is significantly lower (factor 1000)

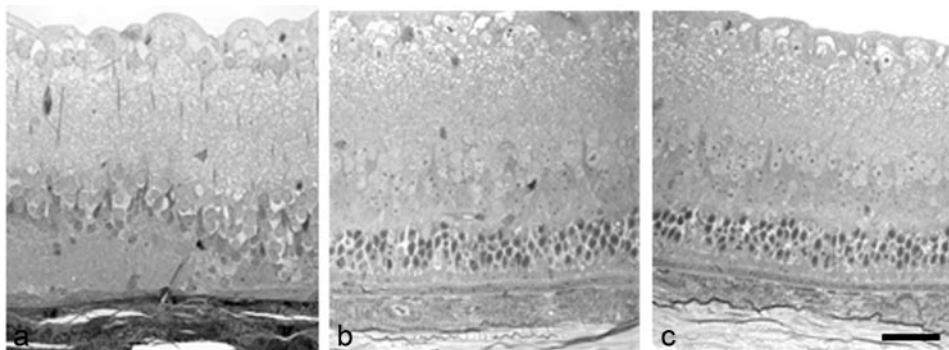


**FIGURE 4.** Semithin sections of RCS rat retinas for the demonstration of rescue effects, the ganglion cell layer is at the *top*. **(a)** In the retina of an untreated control there were no photoreceptor cell nuclei detectable; **(b)** after injection of GFP vector transduced BMSCs there were several rows of preserved photoreceptor cells; **(c)** this tendency continues after transplantation of PEDF vector transduced BMSCs. Scale bar, 30  $\mu\text{m}$ .

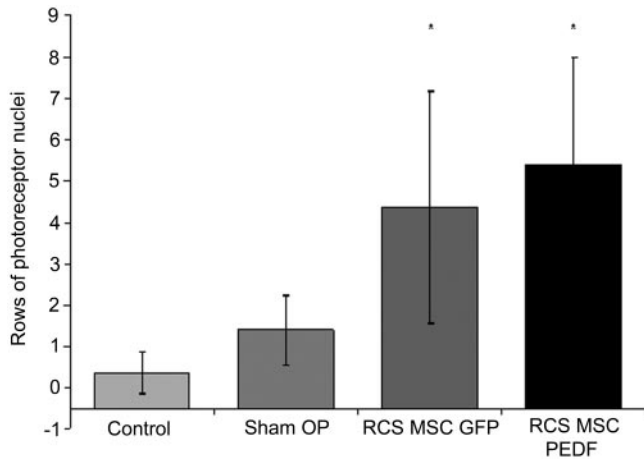


**FIGURE 5.** Quantification and statistical analysis of rescue effects. Quantification of rows of preserved photoreceptor cells per 300- $\mu$ m length of the retina revealed a significant increase after transplantation of both GFP and PEDF vector-transduced BMSCs, compared with the control group. Each experimental group consisted of 10 animals. \*Significant difference versus Sham OP and Control.

than in RPE cells, it may be speculated that other factors synthesized by the bone marrow cells such as BDNF<sup>36</sup> may be responsible for the preserving effect. However, the intrinsic potency of producing PEDF may be a beneficial prerequisite for the transduction of cells using a vector carrying the sequence for PEDF. Consequently, at least regarding the analysis of photoreceptor cells, there is even a slight but not significant increase of the therapeutic effect using PEDF-vector transduced cells. However, there is no clear indication in our study that PEDF also directs differentiation of BMSCs toward RPE cells. The overall limited rescue effects shown in our study using BMSCs derived from adult animals may in fact be attributed to the age of donor cells, similar to the observations by Li and Turner,<sup>35</sup> who used differently aged RPE cells for their therapeutic approach. However, the rescue effects in our study shown on a histologic level, indicate that also BMSCs from adult animals have a benefit in the RCS rat.

Up to now, BMSCs have been shown to differentiate into cells expressing photoreceptor-specific markers such as rhodopsin, opsin, and recoverin in vitro after application of priming factors such as epidermal growth factor (EGF) and activin A, which has been proposed as an approach for the treatment of genetically inherited retinal degenerations.<sup>11</sup> We used unselected BMSCs in our approach. Therefore, it may be specu-

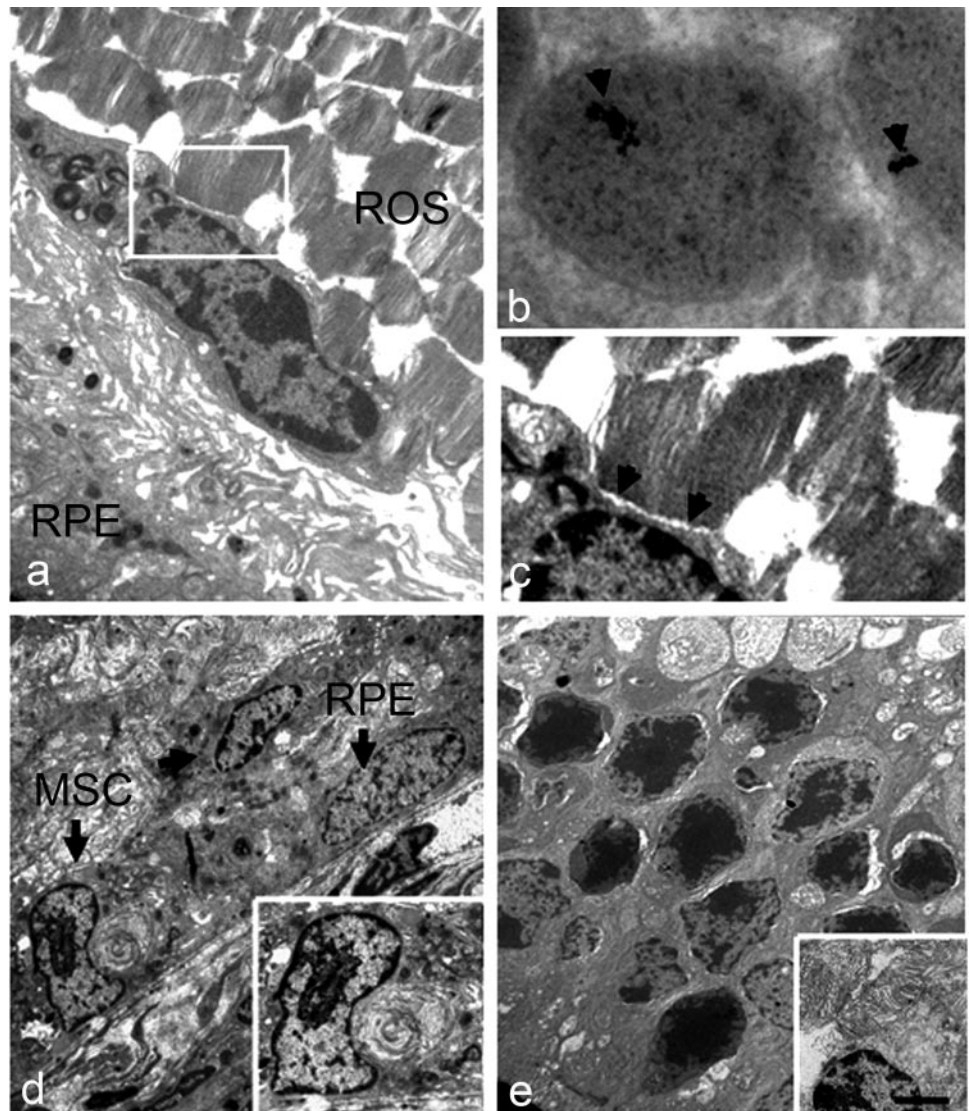


**FIGURE 6.** Ultrastructural analysis of retinas of wild-type and dystrophic RCS rats after MSC injection: (a) After injection into the subretinal space BMSCs, labeled by colloid gold, were situated between the RPE and the photoreceptor outer segments (POS) labeled by colloidal gold. (b) Magnification of (a) to demonstrate the 5-nm gold particles (arrowheads); (c) magnification of the white frame in (a) pointing out the close contacts between rod outer segments and the integrated BMSC (arrowheads). (d) BMSCs after transplantation into the RCS rats on top of the RPE cell layer. BMSCs have taken up phagocytosis of remaining POS. *Inset:* magnification of a BMSC performing phagocytosis. As RPE cells from RCS rats did not phagocytose rod outer segments at all (e), preserved photoreceptor cells after BMSC transplantation in the dystrophic retina; *Inset:* very rarely, preserved inner and outer segments were visible. Scale bars: (a) 2.5  $\mu$ m; (b, c) 0.1  $\mu$ m; (d, e) 5  $\mu$ m; (d, e, insets) 0.7  $\mu$ m.

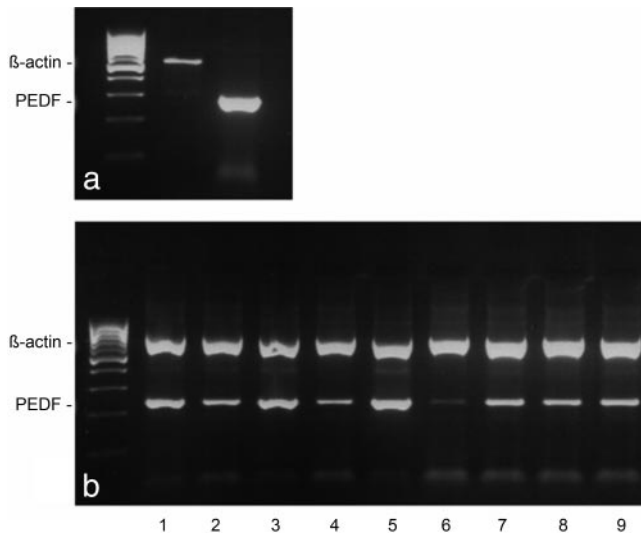


**FIGURE 7.** RT-PCR analysis of PEDF in mesenchymal stem cells. Transcripts of PEDF were detected in (a) rat mesenchymal stem cells as well as (b) in human mesenchymal stem cells of different passages obtained from different patients. The numbers represent different passages from which cells were taken for RNA isolation. Rat  $\beta$ -actin amplicons and human PEDF amplicons generated with intron spanning primers demonstrate the absence of genomic DNA.

lated that without stimulation there is an intrinsic tendency to differentiate into RPE-like cells, rather than into photoreceptor cells. This is consistent with our findings that after transplantation of BMSCs into RCS rats, which means under degenerative conditions, we were able to see a migration of BMSCs into the retina in rare cases, establishing close contacts to host astrocytes. However, an actual transdifferentiation was not observed.

Regarding the use of our technique as a therapeutic option, a possible differentiation into RPE cells is rather promising, as one important function of RPE cells is the phagocytosis of photoreceptor outer segments. Therefore, damage of this cell population leads to photoreceptor degeneration, as has been shown in various animal models for retinal disorders<sup>37,38</sup> as well as in patients with Usher syndrome.<sup>39</sup> In our approach, transplanted BMSCs regularly took up rod outer segment debris, which is an indication that the genetic defect in RCS rats in our study is at least locally rescued.

The use of a high-capacity adenoviral vector that is able to accommodate 36 kb of foreign DNA<sup>40</sup> in conjunction with BMSCs as carrier cells is an important advantage of a combined cell and gene therapeutic approach to the treatment of RPE defects. As the cause of these defects is very often a multifactorial event, probably associated with alterations in more than one gene, a variety of transgenes can be delivered to the lesioned tissue using this vector.

In conclusion, the presented data indicate that, because of their partial morphologic integration, their tendency toward transdifferentiation, and their excellent transduction potential in a third-generation adenoviral vector, autologous BMSCs may serve as carrier cells in a combined cell and gene therapeutic approach in degenerative diseases of the retina, and especially in RPE defects.

### Acknowledgments

The authors thank Jolanta Kozlowski and Hanna Janicki for excellent technical assistance.

### References

1. Devine SM. Mesenchymal stem cells: will they have a role in the clinic? *J Cell Biochem Suppl.* 2002;38:73-79.
2. Lee HS, Huang GT, Chiang H, et al. Multipotential mesenchymal stem cells from femoral bone marrow near the site of osteonecrosis. *Stem Cells* 2003;21:190-199.
3. Lagasse E, Connors H, Al Dhalimy M, et al. Purified hematopoietic stem cells can differentiate into hepatocytes in vivo. *Nat Med.* 2000;6:1229-1234.
4. Shi Q, Rafii S, Wu MH, et al. Evidence for circulating bone marrow-derived endothelial cells. *Blood.* 1998;92:362-367.
5. Orlic D, Kajstura J, Chimenti S, et al. Mobilized bone marrow cells repair the infarcted heart, improving function and survival. *Proc Natl Acad Sci USA.* 2001;98:10344-10349.
6. Ferrari G, Cusella-De Angelis G, et al. Muscle regeneration by bone marrow-derived myogenic progenitors. *Science.* 1998;279:1528-1530.
7. Woodbury D, Schwarz EJ, Prockop DJ, Black IB. Adult rat and human bone marrow stromal cells differentiate into neurons. *J Neurosci Res.* 2000;61:364-370.
8. Kopen GC, Prockop DJ, Phinney DG. Marrow stromal cells migrate throughout forebrain and cerebellum, and they differentiate into astrocytes after injection into neonatal mouse brains. *Proc Natl Acad Sci USA.* 1999;96:10711-10716.
9. Azizi SA, Stokes D, Augelli BJ, DiGirolamo C, Prockop DJ. Engraftment and migration of human bone marrow stromal cells implanted in the brains of albino rats: similarities to astrocyte grafts. *Proc Natl Acad Sci USA.* 1998;95:3908-13.
10. Eglitis MA, Dawson D, Park KW, Mouradian MM. Targeting of marrow-derived astrocytes to the ischemic brain. *Neuroreport.* 1999;10:1289-1292.
11. Kicic A, Shen WY, Wilson AS, Constable IJ, Robertson T, Rakoczy PE. Differentiation of marrow stromal cells into photoreceptors in the rat eye. *J Neurosci.* 2003;23:7742-7749.
12. Strauss O, Stumpff F, Mergler S, Wienrich M, Wiederholt M. The Royal College of Surgeons rat: an animal model for inherited retinal degeneration with a still unknown genetic defect. *Acta Anat (Basel).* 1998;162:101-111.
13. LaVail MM, Sidman RL, Gerhardt CO. Congenic strains of RCS rats with inherited retinal dystrophy. *J Hered.* 1975;66:242-244.
14. Sheedlo HJ, Gaur V, Li LX, Seaton AD, Turner JE. Transplantation to the diseased and damaged retina *Trends Neurosci* 1991;14:347-350.
15. Gouras P, Lopez R, Kjeldbye H, Sullivan B, Brittis M. Transplantation of retinal epithelium prevents photoreceptor degeneration in the RCS rat. *Prog Clin Biol Res.* 1989;314:659-671.
16. Li LX, Turner JE. Inherited retinal dystrophy in the RCS rat: prevention of photoreceptor degeneration by pigment epithelial cell transplantation. *Exp Eye Res.* 1988;47:911-917.
17. Sheedlo HJ, Li L, Gaur VP, et al. Photoreceptor rescue in the dystrophic retina by transplantation of retinal pigment epithelium. *Int Rev Cytol.* 1992;138:1-49.
18. Lawrence JM, Sauve Y, Keegan DJ, et al. Schwann cell grafting into the retina of the dystrophic RCS rat limits functional deterioration. *Invest Ophthalmol Vis Sci.* 2000;41:518-528.
19. Rezaei KA, Kohen L, Wiedemann P, Heimann K. Iris pigment epithelium transplantation. *Graefes Arch Clin Exp Ophthalmol.* 1997; 235:558-562.
20. Schraermeyer U, Kociok N, Heimann K. Rescue effects of IPE transplants in RCS rats: short-term results. *Invest Ophthalmol Vis Sci.* 1999;40:1545-1556.
21. Schraermeyer U, Kayatz P, Thumann G, et al. Transplantation of iris pigment epithelium into the choroid slows down the degeneration of photoreceptors in the RCS rat. *Graefes Arch Clin Exp Ophthalmol.* 2000;238:979-984.
22. Schraermeyer U, Thumann G, Luther T, et al. Subretinally transplanted embryonic stem cells rescue photoreceptor cells from degeneration in the RCS rats. *Cell Transplant.* 2001;10:673-680.
23. Arnhold S, Klein H, Semkova I, Addicks K, Schraermeyer U. Neurally selected embryonic stem cells induce tumor formation after long-term survival following engraftment into the subretinal space. *Invest Ophthalmol Vis Sci.* 2004;45:4251-4255.

24. Dinser R, Kreppel F, Zaucke F, et al. Comparison of long-term transgene expression after non-viral and adenoviral gene transfer into primary articular chondrocytes. *Histochem Cell Biol.* 2001;116:69-77.
25. Barker RA, Widner H. Immune problems in central nervous system cell therapy. *NeuroRx.* 2004;1:472-481.
26. Zarbin MA. Current concepts in the pathogenesis of age-related macular degeneration. *Arch Ophthalmol.* 2004;122:598-614.
27. Houghton J, Stoicov C, Nomura S, et al. Gastric cancer originating from bone marrow-derived cells. *Science.* 2004;306:1568-1571.
28. Aggarwal S, Pittenger MF. Human mesenchymal stem cells modulate allogeneic immune cell responses. *Blood.* 2005;105:1815-1822.
29. Faktorovich EG, Steinberg RH, Yasumura D, Matthes MT, LaVail MM. Photoreceptor degeneration in inherited retinal dystrophy delayed by basic fibroblast growth factor. *Nature.* 1990;347:83-86.
30. Little CW, Castillo B, DiLoreto DA, et al. Transplantation of human fetal retinal pigment epithelium rescues photoreceptor cells from degeneration in the Royal College of Surgeons rat retina. *Invest Ophthalmol Vis Sci.* 1996;37:204-211.
31. Durlu YK, Tamai M. Transplantation of retinal pigment epithelium using viable cryopreserved cells. *Cell Transplant.* 1997;6:149-162.
32. Binder S, Stolba U, Krebs I, et al. Transplantation of autologous retinal pigment epithelium in eyes with foveal neovascularization resulting from age-related macular degeneration: a pilot study. *Am J Ophthalmol.* 2002;133:215-225.
33. Li L, Turner JE. Optimal conditions for long-term photoreceptor cell rescue in RCS rats: the necessity for healthy RPE transplants. *Exp Eye Res.* 1991;52:669-679.
34. Abe T, Yoshida M, Tomita H, et al. Auto iris pigment epithelial cell transplantation in patients with age-related macular degeneration: short-term results. *Toboku J Exp Med.* 2000;191:7-20.
35. Semkova I, Kreppel F, Welsandt G, et al. Autologous transplantation of genetically modified iris pigment epithelial cells: a promising concept for the treatment of age-related macular degeneration and other disorders of the eye. *Proc Natl Acad Sci USA.* 2002;99:13090-13095.
36. Kurozumi K, Nakamura K, Tamiya T, et al. BDNF Gene-modified mesenchymal stem cells promote functional recovery and reduce infarct size in the rat middle cerebral artery occlusion model. *Mol Ther.* 2004;9:189-197.
37. Duncan JL, LaVail MM, Yasumura D, et al. An RCS-like retinal dystrophy phenotype in mer knockout mice. *Invest Ophthalmol Vis Sci.* 2003;44:826-838.
38. Gal A, Li Y, Thompson DA, et al. Mutations in MERTK, the human orthologue of the RCS rat retinal dystrophy gene, cause retinitis pigmentosa. *Nat Genet.* 2000;26:270-271.
39. Gibbs D, Kitamoto J, Williams DS. Abnormal phagocytosis by retinal pigmented epithelium that lacks myosin VIIa, the Usher syndrome 1B protein. *Proc Natl Acad Sci USA.* 2003;100:6481-6486.
40. Kochanek S. High-capacity adenoviral vectors for gene transfer and somatic gene therapy. *Hum Gene Ther.* 1999;10:2451-2459.